# MHD model of accretion disks of young stars

Sergey Khaibrakhmanov*, Alexander Dudorov
Chelyabinsk state university, Chelyabinsk, Russia
*E-mail: khaibrakhmanov@csu.ru

## Introduction

From the fossil magnetic field theory it follows that magnetic flux is partially conserved during star formation, i.e. magnetic field of young stars and their accretion disks is the remnant of the magnetic field of parental protostellar clouds (see for review [1]). Observations supply this hypothesis (Fig. 1). Magnetic field plays crucial role in the process of the angular momentum transport in accretion disks [2]. But intensity and geometry of the large-scale fossil magnetic field is poorly investigated: observations are scanty and theoretical models use prescribed/fixed magnetic field intensity/geometry.

Our main goal is to elaborate MHD model of the accretion disk taking into account main physical effects of ionization and magnetic diffusion [3]. We calculate intensity and geometry of the fossil magnetic field of accretion disks of young stars taking into account Ohmic (OD) and magnetic ambipolar diffusion (MAD).

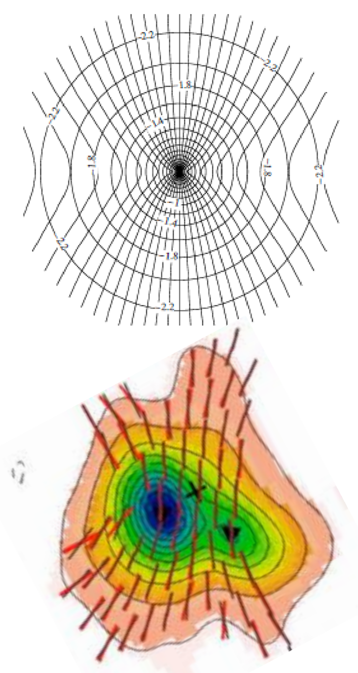

Fig. 1. Magnetic field geometry in collapsing protostellar cloud (top: model [4], bottom: observations [5]).

## Problem statement

We consider geometrically thin optically thick stationary disk. Axial symmetry is assumed. Self-gravitation of the disk is neglected. Disk is in hydrostatic equilibrium. Initial magnetic field – poloidal.

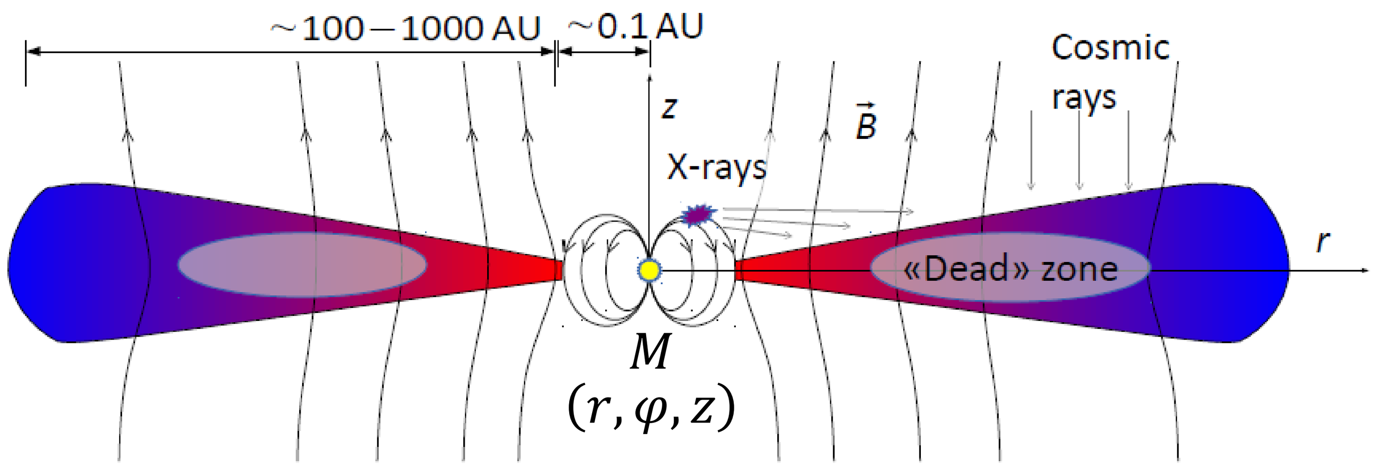


Fig. 2. Schematic view of the accretion disk

$$\vec{V} = (V_r, V_\varphi = \Omega r, 0) \quad \vec{B} = (B_r, B_\varphi, B_z) \quad z \ll r$$

## Basic equations

### I. Disk structure

Temperature $T$, surface density $\Sigma$, scale-height $H$ and radial velocity $V_r$ are calculated from Shakura and Sunyaev equations [6] for given accretion rate $\dot{M}$ and turbulence parameter $\alpha$. Heating due to stellar irradiation is included in (9).

$$\dot{M}\Omega f = 2\pi\alpha\Sigma V_s^2 \quad (1) \qquad \Sigma = 2\rho H \quad (6)$$

$$\dot{M} = -2\pi r V_r \Sigma \quad (2) \qquad V_s = \sqrt{R_g T/\mu} \quad (7)$$

$$\frac{\sigma_{sb}T^4}{3\kappa\Sigma} = \frac{3}{8\pi}\dot{M}\Omega^2 f \quad (3) \qquad \kappa = \kappa_0\rho^a T^b \quad (8)$$

$$H = V_s/\Omega \quad (4) \qquad T_{irr} = 280\,K\left(\frac{L}{L_\odot}\right)^{1/4} r_{AU}^{-1/2} \quad (9)$$

$$\Omega = \sqrt{\frac{GM}{r^3}}\left(1+\frac{z^2}{r^2}\right)^{-3/4} \quad (5)$$

### II. Ionization fraction

Shock ionization fraction $x_s$ is calculated from stationary Spitzer equation (10) taking into account radiative ($\alpha_r$) and dust grain recombinations ($\alpha_g$). Thermal ionization $x_j^T$ is determined from Saha equation (11).

$$(1-x_s)\xi = \alpha_r x_s^2 n + \alpha_g x_s n \quad (10)$$

$$x\frac{x_j^T}{1-x_j^T} = \frac{1}{n}\frac{g_j^+}{g_j^0}\frac{2(2\pi m_e kT)^{3/2}}{h^3}\exp\left(-\frac{\chi_j}{kT}\right) \quad (11)$$

$$x = x_s + \sum_j \nu_j x_j^T \quad \text{j=H, He, Me} \quad (12)$$

Ionization by cosmic rays [7], X-rays [8] and radioactive elements [9] is taken into account.

### III. Magnetic field

Frozen-in vertical magnetic field follows surface density profile (15). Equality of MAD time scale and $B_z$ generation time scale gives (16). Components $B_r$ and $B_\varphi$ are determined from balance between advection of $B_z$ and duffusion in $z$-direction (13-14).

$$B_r = \frac{V_r z}{\eta}B_z \quad (13)$$

$$B_\varphi = \frac{3}{2}\left(\frac{H}{r}\right)^2\frac{V_\varphi z}{\eta}B_z \quad (14)$$

$$B_z = B_{z0}\Sigma/\Sigma_0, \quad (15)$$

$$B_z = (4\pi x\rho^2\eta_{in} r V_r)^{1/2} \quad (16)$$

$$\eta = \frac{c^2}{4\pi\sigma} + \frac{B_z^2}{4\pi x\rho^2\eta_{in}}$$

## Analytical solution

Model equations has analytical solution in case of power-law dependence of ionization fraction on density $x_s \propto n^{-q}$. E.g., for dust grain recombinations $q = 1$, ionization fraction and vertical magnetic field (in case of efficient MAD) profiles are (for $\kappa = 3.0\times10^{-3}T\ \mathrm{cm^2/g}$)

$$x_g = 3.4\times10^{-15}\left(\frac{\xi}{10^{-17}\ \mathrm{s^{-1}}}\right)\left(\frac{\alpha}{0.01}\right)^{5/8}\left(\frac{\dot{M}}{10^{-8}M_\odot/\mathrm{yr}}\right)^{-7/16} \times\left(\frac{M}{1M_\odot}\right)^{-1/4}\left(\frac{r}{1\ \mathrm{AU}}\right)^{-21/16} \quad (17)$$

$$B_z^{mad} = 0.024\left(\frac{\xi}{10^{-17}\mathrm{s^{-1}}}\right)^{1/2}\left(\frac{\alpha}{0.01}\right)^{1/16}\left(\frac{\dot{M}}{10^{-8}M_\odot/\mathrm{yr}}\right)^{3/8} \times\left(\frac{M}{1M_\odot}\right)^{5/32}\left(\frac{r}{1\ \mathrm{AU}}\right)^{-15/32}\mathrm{Gs} \quad (18)$$

## Fossil magnetic field geometry

In general case, non-linear model equations are solved by iterative methods. Here we analyze $B_r(r,H), B_\varphi(r,H), B_z(r,H)$ profiles (Fig. 3) and 2D disk structure (Fig. 4) for typical solar-mass T Tauri star [10], $\dot{M} = 10^{-8}M_\odot/\mathrm{yr}$, $\alpha = 0.01$, $L = 1L_\odot$, $B_s = 2\mathrm{kGs}$, $R_s = 2R_\odot$, $L_{XR} = 10^{30}\mathrm{erg/s}$

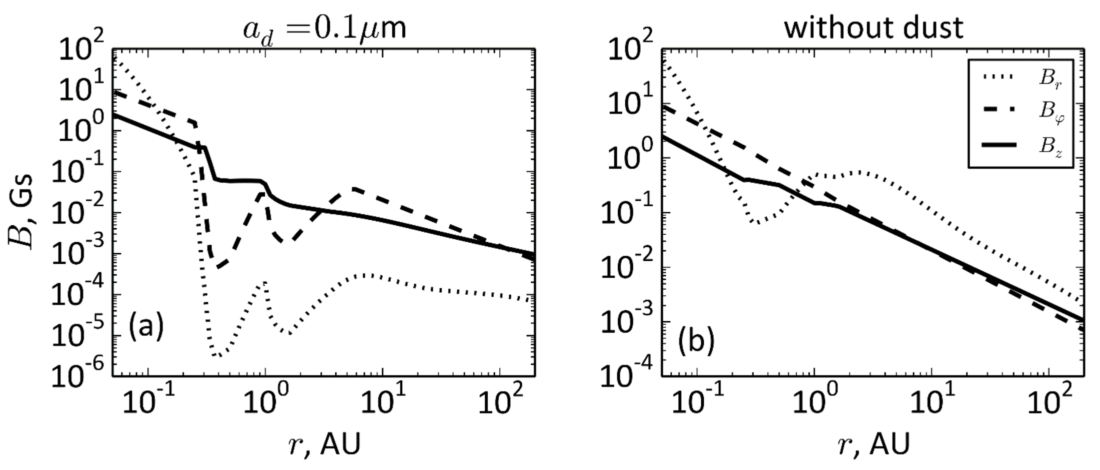


Fig. 3. Radial profiles of the magnetic field components at height $H$ (a: dust size is 0.1 $\mu m$, b: without dust).

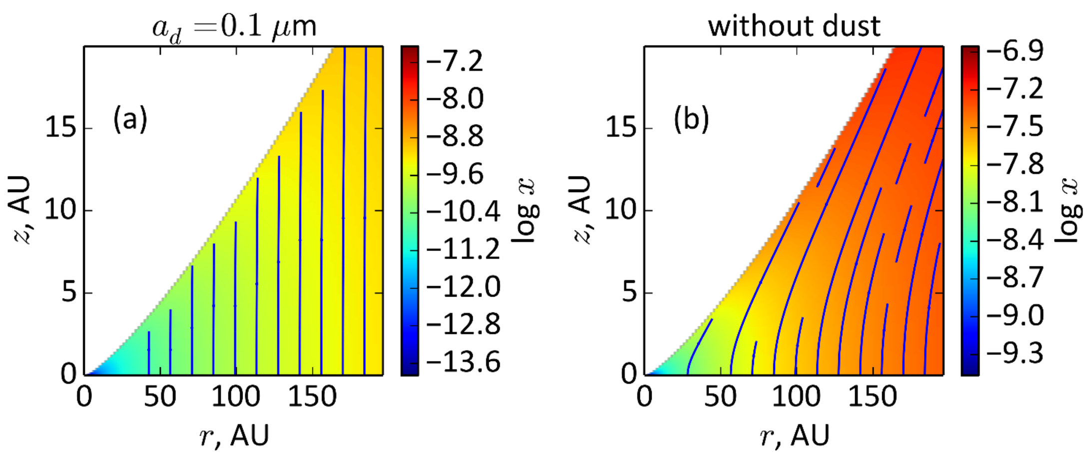


Fig. 4. 2D accretion disk structure (a: dust size is 0.1 $\mu m$, b: without dust). Color: ionization fraction, blue lines: poloidal magnetic field lines.

Fig. 3a show that magnetic field is quasi-azimuthal ($B_\varphi \gg B_r, B_z$) at $r < 0.3$ AU, quasi-poloidal ($B_z \gg B_r, B_\varphi$) at 0.3-10 AU (region of small ionization fraction and efficient Ohmic diffusion – "dead" zone [11]) and quasi-azimuthal at $r > 10$ AU. In absence of dust (Fig. 3b, 4b) magnetic field is frozen-in and all three components are comparable. In this case inclination of poloidal magnetic field lines is sufficient to form centrifugally driven wind.

## "Dead" zones

We calculated boundaries ($r_{in}^{dz}$ and $r_{out}^{dz}$) and masses ($M_{dz}$) of the "dead" zones using criterion from [9]. Calculations show that MAD determines outer boundary of the "dead" zone.

| $\frac{M}{M_s}$ | $\frac{r_{in}}{\mathrm{AU}}$ (disk) | $\frac{r_{out}}{\mathrm{AU}}$ | $\frac{M_{disk}}{M_s}$ | $\frac{r_{in}^{dz}}{\mathrm{AU}}$ | | $\frac{r_{out}^{dz}}{\mathrm{AU}}$ | | $\frac{M_{dz}}{M_J}$ | |
|---|---|---|---|---|---|---|---|---|---|
| 0.5 | 0.085 | 70 | 0.003 | 0.11 | 0.14 | 3.1 | **2.8** | 0.04 | **0.02** |
| **1** | **0.052** | **140** | **0.027** | **0.26** | **0.32** | **10.7** | **13.7** | **0.8** | **1.0** |
| 1.5 | 0.039 | 210 | 0.1 | 0.43 | 0.55 | 16.3 | **19.0** | 3.6 | **4.1** |
| 2 | 0.032 | 270 | 0.17 | 0.6 | 0.75 | 17.2 | **21.4** | 5.0 | **5.9** |
| Table 1. | | | | OD | MAD | OD | **MAD** | OD | **MAD** |

## Conclusion

The fossil magnetic field of accretion disks of young stars has complex geometry. It is qiasi-poloidal in the dusty "dead" zones due to Ohmic diffusion. Outer boundary of the "dead" zone is determined by the magnetic ambipolar diffusion. Magnetic field is quazi-azimuthal or quasi-radial ($B_z \approx B_r$) outside the "dead" zone depending on intensity of ionization mechanisms. In presence of dust, magnetic ambipolar diffusion prevents generation of radial magnetic field component in the outer regions. Mass of solid material inside "dead" zones in accretion disks of stars with $M \geq 1M_\odot$ is more than $3M_\oplus$. This mass is sufficient for formation of several embryos of the Earth type planets.

## References

1. Dudorov, Khaibrakhmanov, AdSpRes, DOI:10.1016/j.asr.2014.05.034 (2014)
2. Turner, et al., eprint arXiv:1401.7306
3. Dudorov, Khaibrakhmanov, ApSS, 352(1), 103 (2014)
4. Dudorov, Zhilkin, ARep, 52(10), 790 (2008)
5. Girart, Rao & Marrone, Sci, 313, 812 (2006)
6. Shakura & Sunyaev, A&A, 24, 337 (1974)
7. Spitzer & Tomasko, ApJ, 152, 971 (1968)
8. Bai & Goodman, ApJ, 701, 737 (2009)
9. Sano, et al., ApJ, 543, 486 (2000)
10. Williams & Cieza, A&A, 49, 67 (2011)
11. Gammie, ApJ, 457, 355 (1996)